Anionic lipids and the cytoskeletal proteins MreB and RodZ define the spatio-temporal distribution and function of membrane stress controller PspA in *Escherichia coli*

Goran Jovanovic[1,*], Parul Mehta[1], Liming Ying[2] and Martin Buck[1,*]

[1]*Department of Life Sciences, Imperial College London, London SW7 2AZ, United Kingdom;* [2]*National Heart and Lung Institute, Imperial College London, London SW7 2AZ, United Kingdom*

[*]*Correspondence: Goran Jovanovic and Martin Buck. G.J., Department of Life Sciences, Faculty of Natural Sciences, Room 522, SAFB, Imperial College Road, Imperial College, London SW7 2AZ, UK; Tel. +44(0)2075941235; Fax. +44(0)2075945419; E-mail g.jovanovic@imperial.ac.uk. M.B., Department of Life Sciences, Faculty of Natural Sciences, Room 448, SAFB, Imperial College Road, Imperial College, London SW7 2AZ, UK; Tel. +44(0)2075945442; Fax. +44(0)2075945419; E-mail m.buck@imperial.ac.uk*

Running title: Inner membrane stress control

Keywords: inner membrane stress; PspA; cardiolipin; signal-transduction; bacterial actin; cell wall biosynthesis.

Abbreviations: Psp, Phage shock protein; IM, inner membrane; pmf, proton motive force; pIV, phage f1 protein IV (secretin); WT, wild type; CL, cardiolipin; PG, phosphatidylglycerol; PGL, peptidoglycan; SMI, single molecule imaging; V, fluorescent protein venus; eGFP, enhanced green fluorescent protein; TIRF, total internal reflection fluorescence.

Word count: 7591; Total number of figures: 6.

Abstract

All cell types must maintain the integrity of their membranes. The conserved bacterial membrane-associated protein PspA is major effector acting upon extracytoplasmic stress and is implicated in protection of the inner membrane of pathogens, formation of biofilms and multi-drug resistant persister cells. PspA and its homologues in Gram-positive bacteria and archaea protect the cell envelope whilst also supporting thylakoid biogenesis in cyanobacteria and higher plants. In enterobacteria, PspA is a dual function protein negatively regulating the Psp system in the absence of stress and acting as an effector of membrane integrity upon stress. We show that in *Escherichia coli* the low-order oligomeric PspA regulatory complex associates with cardiolipin-rich, curved polar inner membrane regions. There, cardiolipin and the flotillin 1 homologue, YqiK, support the PspBC sensors in transducing a membrane stress signal to the PspA-PspF inhibitory complex. After stress perception, PspA high order oligomeric effector complexes initially assemble in polar membrane regions. Subsequently, the discrete spatial distribution and dynamics of PspA effector(s) in lateral membrane regions depends on the actin homologue MreB and peptidoglycan machinery protein RodZ. The consequences of loss of cytoplasmic membrane anionic lipids, MreB, RodZ and-or YqiK suggest that the mode of action of the PspA effector is closely associated with cell envelope organisation.

INTRODUCTION

Maintaining membrane integrity is fundamental to all cell types and of key importance to energy production, signalling, adaptation to the environment and cellular compartmentalisation. Many Gram-negative bacteria mount a major adaptive response to extracytoplasmic stress by inducing the Phage shock protein (Psp) system (reviewed in Model *et al*., 1997; Darwin, 2005; Joly *et al*., 2010). Related stress control systems are found in Gram-positive bacteria, cyanobacteria, archaea and in higher plants (Joly *et al*., 2010).

The Psp system of Gram-negative bacteria is induced by a variety of membrane stress stimuli such as protein translocation defects (Joly *et al*., 2010; Wang *et al*., 2010; Wickström *et al*., 2011) and production of secretins, e.g., pIV, PulD, YscC, OutD, that are components of the types II, III and IV secretion systems (reviewed in Joly *et al*., 2010; Yamaguchi & Darwin, 2012). The Psp response of bacterial pathogens protects the cell envelope during infection and is important for biofilm formation and virulence whilst also being implicated in antibiotic resistance and formation of persister cells (reviewed in Joly *et al*., 2010; Darwin, 2013; see also Dhamdhere & Zgurskaya, 2010; Vega *et al*., 2013; Wallrodt *et al*., 2014). Agents inducing *psp* impair the plasma membrane and dissipate the proton motive force (pmf). A drop in pmf may not be sufficient to induce the Psp response and multiple signals appear to be integrated to induce the response in enterobacteria (Wang *et al*., 2010; Engl *et al*., 2011). The highly conserved bacterial peripheral membrane protein PspA acts as a major effector which, through a yet unknown mechanism, repairs the membrane and so preserves the pmf (Joly *et al*., 2010). Homologues of PspA in *Mycobacterium* and other Gram-positive bacteria (e.g. LiaH in *Bacillus*) have been postulated to maintain cell wall homeostasis upon extracytoplasmic stress (Joly *et al*., 2010; White *et al*., 2011; Darwin, 2013) to confer resistance to cell wall/peptidoglycan (PGL) and membrane integrity targeting antibiotics (reviewed in Jordan *et al*., 2008; Joly *et al*., 2010). In cyanobacteria and plants, the PspA homologue VIPP1 is required for photosynthesis through support of thylakoid membrane biogenesis and protection of the cell envelope (Westphal *et*

al., 2001; Aseeva *et al*., 2004; Aseeva *et al*., 2007; Vothknecht *et al*., 2012; Zhang *et al*., 2012; Zhang & Sakamoto, 2013).

PspF, PspA, PspB and PspC are conserved in enterobacteria and constitute the core proteins of the Psp response (Huvet *et al*., 2011). Under non-stress conditions in enterobacteria, σ^{54}-RNA polymerase dependent *psp* expression is negatively regulated by PspA *via* its direct ~1:1 binding to the surface exposed hydrophobic 'W56 loop' of the hexameric bacterial enhancer-binding protein PspF (Joly *et al*., 2009; Zhang *et al*., 2013). Under inner membrane (IM) stress, induction of *psp* involves the IM-bound PspB and PspC proteins sensing stress and recruiting PspA-PspF inhibitory complex to the IM (Jovanovic *et al*., 2010; Yamaguchi *et al*., 2010). Relieving the inhibition of PspF imposed by PspA involves changing PspA interacting partners from PspF to PspBC, resulting in strong induction of *psp* genes and formation of PspA effector complexes at the IM (Yamaguchi *et al*., 2013; Mehta *et al*., 2013). Upon stress, σ^{70}-controlled expression of PspF remains unchanged (Lloyd *et al*., 2004).

Single molecule sensitivity imaging (SMI) studies of chromosome expressed fluorescent fusion Venus-PspF in live *Escherichia coli* cells established that the PspF is predominantly hexameric and that the PspA-Venus-PspF nucleoid-bound inhibitory complex under non-stress conditions communicates with the IM in a PspA and PspBC-dependent manner (Mehta *et al*., 2013). Under IM stress, PspF is stably bound to the nucleoid and involved in transcription while Venus-PspA (or eGFP-PspA) is found within static polar and dynamic lateral IM complexes. Static polar IM complexes correlate with a PspA regulatory function within the signalling complex PspA-PspBC, while the dynamic lateral IM complexes correlate with PspA effector function (Engl *et al*., 2009; Jovanovic *et al*., 2014). When the dynamics of lateral membrane eGFP-PspA complexes is abolished or when PspA is mutated so it can interact with the PspF and PspBC but cannot bind the IM and form the lateral membrane complexes, the PspA is able to form the polar IM complexes and respond to PspBC-dependent IM stress but is unable to e.g. conserve the pmf. The major oligomerisation state of eGFP-PspA found in static polar foci is a 6-mer with a minority of additional high-order oligomers up

to ~36-mer (Lenn *et al*., 2011). Relief of negative control results in a PspA binding to the IM, switch in oligomeric state from low-order to high-order oligomers and the appearance of lateral IM PspA effector complexes (Jovanovic *et al*., 2014). These observations suggest that a switching mechanism linked to the stress signalling pathway in cellular polar membrane regions exists to convert PspA between its negative regulator (potentially 6-mer) and effector (36-mer) forms. Apparently, PspBC, as opposed to PspA, have a direct secretin-damage effector function in *Y. enterocolitica* (PspC has extra amino acids at its N-terminus compared to the *E. coli* PspC) (Hortman & Darwin, 2012). Moreover, Yamaguchi *et al*. (2013) did not observe lateral IM PspA effector complexes upon stress suggesting that action of PspA effectors in stressed *Y. enterocolitica* cells might be orchestrated differently from *E. coli*. Nevertheless, at the same time it was established that static polar PspBC sensors co-localise with PspA at the onset of stress, consistent with the polar PspA-PspBC complexes functioning in a regulatory manner in *E. coli*.

Impaired phospholipid biosynthesis is a strong inducer of PspA in *E. coli* (Bergler *et al*., 1994). In turn, Kobayashi *et al.* (2007) provided evidence that the higher oligomeric form (36mer) of purified PspA acts as an effector which binds phosphatidylglycerol (PG) and prevents proton leakage from membrane vesicles. In *E. coli*, the major phospholipid is phosphatidylethanolamine (~75% of total IM lipids) which possesses a zwitterionic head group. The most abundant anionic IM phospholipids implicated in signalling and-or functioning of IM proteins are PG (~20% of total IM lipids) and dianion cardiolipin (CL) (~5% of total IM lipids) (reviewed in Foss *et al*., 2011). The polar and lateral regions of the IM are rich in PG whilst the majority of CL resides in polar regions (Foss *et al*., 2011) (see Supplementary Fig. S1a). Although PspA effector complexes do not directly bind CL *in vitro* (Kobayashi *et al*., 2007), the position of the PspBC-dependent PspA regulatory complexes close to poles imply that CL and or negative curvature might be involved in localisation and function of the PspBC sensors and or PspA-PspBC complexes. Indeed, the function of e.g. Tat protein translocation system is CL-dependent (reviewed in Arias-Cartin *et al*., 2012; Berthelmann & Brüser, 2004), and PspBC-PspA-Tat direct interactions have been reported (Mehner *et al*., 2012).

MreB is a bacterial actin and a key component of the bacterial cytoskeleton (reviewed in Typas *et al*., 2012). The helix-like circumferential dynamics and function of lateral IM PspA effector complexes depends on MreB in *E. coli* (Engl *et al*., 2009). In *E. coli* MreB assembles into short filaments that either bind directly to the cell membrane via the N-terminal amphipathic helix and move as independent units in directions that are perpendicular to the long axis of the cell (Salje *et al*., 2011) or co-localises and interacts with RodZ (van den Ent *et al*., 2010) and organises the cell wall (PGL) synthesis machinery assembly coupling their rotation in a helix-like circumferential fashion (van Teeffelen *et al*., 2011) (see Supplementary Fig. S1b). The PG-dependent lipid helices were observed in Gram-negative and Gram-positive bacteria (Barák *et al*., 2008). Since PspA as an effector binds PG *in vitro* and PspA and PspB interact with MreB *in vivo* (Engl *et al*., 2009), the spatial organisation and dynamics of PspA, MreB and anionic lipids might be interlinked. These relationships could be important in response to physico-chemical changes of the IM relevant to regulation and functioning of the Psp system.

In this study we applied genetic tools in combination with SMI to explore *in vivo* how PspA communicates with the IM stress signalling pathways and undergoes a switch from being a negative regulator to acting as an effector. We established a link between CL and induction of the Psp response on one hand and the bacterial cytoskeleton and effector functions of PspA on the other. Our results provide evidence that membrane curvature, membrane lipid composition, bacterial actin MreB and cell wall biosynthesis machinery affect the dynamics of PspA upon IM stress.

METHODS

Bacterial strains, plasmids and growth conditions. Bacterial strains and plasmids used in this work are listed in Supplementary Table S1. New strains were constructed using $P1_{vir}$ transduction (Miller, 1992) (e.g. MG1655xMVA127 results in a strain MVA101; see Supplementary Table S1). All strains were routinely grown under microaerobic conditions in Luria-Bertani (LB) broth or on LB agar plates at 37°C (Miller, 1992). For microaerobic growth, overnight cultures of cells were diluted 100-fold (to

an OD_{600nm}~0.025) and shaken in universals at 100 rpm. For SMI of eGFP-PspA and Venus-PspA (V-PspA), cells were grown in N^-C^- minimal medium supplemented with 0.4% (w/v) glucose as carbon source, 10 mM NH_4Cl as nitrogen source, and trace elements at 30°C as described (Engl *et al*., 2009; Mehta *et al*., 2013). The expression of pIV from pMJR129 was induced by 1 mM IPTG for 10 or 20 min. The expression from pCA24N-based constructs (JW plasmids, see Supplementary Table S1) was induced by 0.1 mM IPTG for 1 hour. The expression of eGFP-PspA and the expression of pIV from pGJ4 were leaky and constitutive. Antibiotics used: ampicillin (100 μg ml^{-1}), kanamycin (25 or 50 μg ml^{-1}, as indicated) chloramphenicol (30 μg ml^{-1}), tetracycline (10 μg ml^{-1}) and fosfomycin (16, 32 or 64 μg ml^{-1}, as indicated).

***In vivo* assays.** The activity of chromosomal transcription fusion ϕ(*pspA-lacZ*) was measured using the β-Galactosidase (β-Gal) assay as described (Miller, 1992). For the β-Gal assay, overnight cultures grown at 37°C were diluted 100-fold and grown under the same conditions until mid-log phase. The β-Gal data for all assays shown (except for the experiments with fosofomycin) are presented as the mean values (with S.D. error bars) of measurements of six samples (technical duplicates of three independently grown cultures of each strain).

For the experiment using fosfomycin, wild type (WT) or WT+pIV cells were grown as above until mid-late log phase and then each day culture was separated into five. The separate samples were inoculated with 0, 16 and 32 μg ml^{-1} (1 MIC=64 μg ml^{-1}) of fosfomycin, incubated for additional 10 min at 37°C and then assayed for β-Gal activity. The β-Gal data are presented for each of the three independent experiments.

The growth of WT and different mutants under non-stress or stress (pIV production) was measured in LB at 37°C. The OD_{600nm} of overnight cultures was measured and cultures densities were than standardised to OD_{600}=0.025 at t=0, after inoculation into 20 ml of LB and then shaken at 100 rpm at 37°C. The cells were taken for measurements of cell growth at OD_{600} and colony forming units (CFU)

at hourly intervals (1-7 hours). The data presented are from a single experiment in which all strains were tested simultaneously. The growth of strain from three independent assays was compared to either an isogenic strain carrying the control vector plasmid or (for the mutants) to the WT parent strain before and after stress.

For cell growth and fosfomycin LacZ expression experiments, the statistical significance of differences between strains was determined using Students T-test. P-value less than 0.05 is considered as a significant.

Proteins. Expression of V-PspA and pIV was determined using antibodies against Venus [JL-8 Living Colours (Clonetech); (1:5,000)] and pIV (1:1,000), respectively, and Western blotting. The Western blot analyses were performed on a Bench Pro^{TM} 4100 Card processing station (Invitrogen). Proteins were detected using the ECL plus Western Blotting Detection Kit (GE Healthcare) and images were visualised using Bio-Rad GelDoc^{TM} and ChemiDoc^{TM} Imaging system with Image Lab software. The quantitative analyses were performed using ImageJ software.

Microscopy and imaging data analyses. Cells expressing plasmid borne eGFP-PspA or chromosomal fusion of V-PspA were grown at 30^{o}C in minimal media (see above). The live cells were immobilized on 1% agarose pads set on a glass slide surface as described (Engl *et al*., 2009). For the experiment where the V-PspA expression was analysed after 10 or 20 min induction of pIV, IPTG (1 mM final) was added directly to the agarose pads simultaneously with the cells. V-PspA was visualised using wide field epifluorescence microscopy. The expression of pIV was tested independently in the same samples grown in media (0, 10 or 20 min) using Western blot and pIV antibodies (see above). For the experiment with fosfomycin the stressed Δ*pspA* cells expressing V-PspA were grown to OD_{600}~0.8, treated with 32 μg ml^{-1} of fosofomycin for 10 min at 37^{o}C and imaged. The wide field or TIRF SMI of live bacterial cells using a custom-built inverted epifluorescence/TIRF microscope based on a Nikon TE2000 optical system was as described (Mehta

et al., 2013). TIRF microscopy was employed to limit the laser penetration up to ~50-100 nm into the bacterial cell in order to differentiate between nucleoid and membrane associated V-PspA foci. The axial resolution for wide field imaging is ~1 μm so that an entire *E. coli* cell with diameter ~500 nm was imaged; hence the foci within the same/similar Z (e.g. nucleoid-associated and polar membrane) can be in focus. The exposure time was 38 milliseconds (ms) (for eGFP) or 15 ms (for Venus). A 100-1000 frame video sequence with 2x2 binning at a frame interval of 25 ms (for eGFP) or 30 ms (for Venus) was recorded. The Deltavision OMX V3 system (Applied Precision, Washington) with 3 ms exposure time at a frame interval of 44 ms was used for photobleaching experiments of the rare V-PspA static foci observed in the nucleoid under non-stress conditions and of V-PspA foci at the poles under non-stress or stress conditions. Photobleaching traces of individual V-PspA static nucleoid foci under non-stress conditions and polar foci from non-stress and stressed cells were analysed and the oligomeric states were determined as described (Lenn *et al*., 2011; Mehta *et al*., 2013). The images were analysed using ImageJ (www.rsbweb.nih.gov/ij/) and FiJi. The quantitative analysis of localisation of V-PspA foci in the cell, the quantification of number of foci per cell and the total raw intensity profiles was performed using ImageJ software. Cells expressing eGFP-PspA or V-PspA were analysed to determine the intensity of foci at specific cellular locations. For the spatial analysis of signal, a line of approximately 18 pixels wide was drawn along the longitudinal axis of cells of similar lengths to cover the entire cell and the intensity values were obtained yielding pixel by pixel intensity value across the cell length from pole to pole. When the differences in intensity values were high, for comparison we normalised the data points representing the mean intensity. The apparent 2-dimension diffusion analysis (diffusion coefficient D) of V-PspA foci determined using Matlab (Mathwork) scripts was as described (Mehta *et al*., 2013).

RESULTS

The IM stress causes formation of V-PspA high order oligomers in polar membrane regions and increase of V-PspA complexes in lateral membrane

To assess and quantify the spatial and temporal dynamics of V-PspA under increasing IM stress conditions, we used a strain lacking the native *pspA* gene and expressing chromosomal single copy P_{pspA}-V-PspA (Mehta *et al*., 2013; see also Fig. 1a) in the absence or presence of increasing amounts of the pIV. pIV is the other membrane secretin which mislocalisation into the IM induces the PspBC-dependent Psp response (Joly *et al*., 2010). The V-PspA (or eGFP-PspA) fusion exhibits reduced (50%) negative control activity compared to WT PspA (Engl *et al*., 2009; Mehta *et al*., 2013) and this accounts for the moderately elevated expression of both V-PspA and PspBC under non-stress conditions in a Δ*pspA* strain (Jovanovic *et al*., 2014). Consequently, in wide field SMI we observe V-PspA complexes (2±0.3 foci per cell, n=50) in the polar region of the cell and some lateral membrane foci (Fig. 1b; Supplementary Video S1). The pIV induced IM stress and its time-dependent increase (Fig. 1f) lead to a gradual elevation in total fluorescence intensity of V-PspA (Fig. 1g) and increased number of dynamic and static lateral V-PspA complexes (Fig. 1c, d, g; Supplementary Video S2 and S3). Notably, V-PspA expression, localisation and dynamics in stressed cells closely resemble those of plasmid borne eGFP-PspA as expressed in non-stressed Δ*pspA* cells (Fig. 1e, g; Supplementary Video S4).

The total fluorescence intensity represents the number of V-PspA molecules. The very significant increase in total fluorescence intensity between 10 and 20 min induction of pIV (Fig. 1g, left hand) reflects a moderate increase in pIV level (Fig. 1f) and a small increase in the number of lateral V-PspA foci (10 min – 7±0.6, 20 min – 8±0.7, n=50) (see also Fig. 1g, right hand). However, the formation of foci containing high-order oligomeric V-PspA effectors may be the main factor contributing to total fluorescence intensity.

Using wide-field SMI and photobleaching we determined the oligomeric states of V-PspA under non-stress or stress growth conditions. In the non-stressed state V-PspA imaged as low-order (3-10mer) assemblies in rare central static nucleoid-associated foci (Fig. 2a), presumably interacting with PspF and forming a PspA-PspF inhibitory complex at *psp* promoter(s) as shown by Mehta *et al*. (2013).

This is in good agreement with *in vitro* data establishing that at least 3 PspA proteins are necessary to bind PspF for negative control (Zhang *et al*., 2013). We also determined that in non-stressed cells V-PspA is a low-order assembly in polar foci likely representing the PspA-PspBC membrane regulatory complexes (Fig. 2b). During stress, the V-PspA in polar complexes is found as both low (5-6 up to 12mer) and high-order assemblies (up to 25mer; photobleaching and maturation of Venus fluorescence protein may limit the observed number of V-PspA subunits, especially in foci representing high-order oligomers) (Fig. 2b). It seems that the IM stress signals lead to a distinct dynamic response following an increase in V-PspA expression and its high-order oligomer formation in polar membrane regions.

The efficient PspA negative control is required for native basal level expression and spatial distribution of V-PspA

To determine the behaviour of V-PspA when expressions of PspBC are natively controlled, the P_{pspA}-V-PspA was integrated as a single chromosomal copy into the WT cells expressing native PspA (Fig. 3a). Normal regulation of *psp* expression characterised by a low level of stable V-PspA under non-stress conditions was observed whereas elevated levels were seen in pIV stressed cells (Fig. 3b). When V-PspA and native PspBC are expressed at a basal level in non-stressed WT cells V-PspA localise either as a single nearly static central nucleoid [by means of interacting with PspF (Mehta *et al*., 2013; Jovanovic *et al*., 2014); visible in wide field but not visible in TIRF] or as a static polar membrane complex (visible in both wide field and TIRF) (Fig. 3c). This is in agreement with Venus-PspF (V-PspF) imaging in live cells revealing a single central nucleoid V-PspF-PspA inhibitory complex that communicates in a PspBC-dependent fashion with the polar membrane region by fast relatively free diffusion (Mehta *et al*., 2013). Under stress, when expression of V-PspA is induced, we observed polar regulatory complexes and the appearance of static and dynamic lateral effector V-PspA complexes (Fig. 3d; Supplementary Video S5). Therefore, with the negative control imposed by native PspA we can clearly visualise V-PspA exhibiting the “off” and “on” state of the Psp response.

Cardiolipin is implicated in a PspBC-dependent induction of the Psp response

The anionic phospholipid cardiolipin (CL) has mainly a membrane curvature associated polar localisation (Renner & Weibel, 2011). PspA does not appear to bind membrane vesicles containing CL (Kobayashi *et al*., 2007) but PspA is tethered by and co-localises with static PspBC foci in curved polar membrane regions (Yamaguchi *et al*., 2013; Mehta *et al*., 2013). This suggests that localisation of the inhibitory PspA-PspF complex or PspA within PspA-PspBC regulatory complex at the poles of cells may depend on PspA interacting with the PspBC bound to CL-rich membrane domains. We examined the contribution of CL to PspA activities and to cell growth under IM stress in a Δ*cls* mutant (non-polar mutation) containing a significantly reduced amount of CL (Brandon *et al*., 2012).

We determined that Δ*cls* mutation does not induce the Psp response *per se* and actually decreases either basal level expression or induction of *pspA* under stress (Fig. 4a). In addition, the induction of *pspA* under stress is to some extent PspBC-independent in a Δ*cls* mutant (Fig. 4a). In the absence of negative control in Δ*pspA* cells the Δ*cls* mutation does not impact on σ^{54}-dependent transcription of *pspA* gene (Supplementary Fig. S2a), suggesting that observed differences in *pspA* expression in Δ*cls* cells reflect a change in the PspA negative control function. Additionally, the over-expression of either PgsA implicated in biosynthesis of PG and CL or Cls required for CL biosynthesis does not induce the Psp response (Supplementary Fig. S2b). We note that over-expression of phospholipid synthases had little impact on the overall pool of individual phospholipids within *E. coli* (reviewed in Raetz, 1986).

Growth in a stressed Δ*cls* mutant is delayed but the final growth yield is not significantly reduced compared to WT cells (Fig. 4b). As a control, a Δ*pspF* mutant lacking any induction of the Psp response exhibits growth that is severely impaired (Fig. 4c). Notably, the increased amount of PG seen in a Δ*cls* mutant (Brandon *et al*., 2012) and the fact that PspA effectors bind PG may account for cell adaptation and normal growth upon IM stress, even though the induction of Psp response is decreased in a Δ*cls* cells.

To determine whether CL affects the sub-cellular localisation of V-PspA, we imaged V-PspA in an *E. coli* Δ*cls* mutant background under non-stress or stress conditions using the wide field and TIRF modes of SMI. The majority of non-stressed Δ*cls* cells show only nucleoid-associated V-PspA (100%, n=50, of mostly central foci not visible in TIRF) and no polar regulatory complexes (Fig. 4d) in agreement with increased negative control of PspF (Fig. 4a). Under stress, in Δ*cls* cells we observe the appearance of lateral V-PspA foci but the number of polar complexes is significantly reduced compared to the WT (Fig. 4e, g and Supplementary Video S6 and Fig. S3a, b). The total intensity of V-PspA foci in stressed Δ*cls* cells (Supplementary Fig. S3c) correlates well with the level of *pspA* induction upon stress (Fig. 4a) and the amount of effector complexes is in accordance with their growth being close to WT (Fig. 4b). As seen for the PspBC- and CL-independent induction of *pspA* (Fig. 4a), stressed Δ*pspBC* Δ*cls* cells induce the expression of V-PspA and the formation of the lateral effector but not polar complexes can be readily observed (Fig. 4f).

Although we failed to construct a stable and functional PspB or PspC-eGFP/Venus fusion protein to directly localise the Psp sensor(s) in a WT or *cls* mutant, it is established that PspBC recruits PspA-V-PspF complex to the IM in *E. coli* and co-localise with PspA in polar membrane region of *Y. enterocolitica* cells (Yamaguchi *et al*., 2013). Therefore, our results strongly suggest that the PspBC-dependent induction of the Psp response under stress and the localisation of V-PspA within polar IM regulatory complexes are influenced by the presence of CL.

Apparently, CL depletion affects the membrane in numerous ways (reviewed in Arias-Cartin *et al*., 2012) and could therefore indirectly influence PspB and PspC activity. Relevant to the Psp response, CL-associated flotillin YuaG (FloT) from *Bacillus subtilis* functionally organises the bacterial membrane and interacts with proteins involved in membrane-related signaling and protein secretion (Donovan & Bramkamp 2009; Bach & Bramkamp, 2013). However, PspA homologue LiaH or its regulator(s) has not been found to interact with YuaG. Intriguingly, there is a potential flotillin 1

homologue in *E. coli*, an inner membrane protein YqiK, which might act in scaffolding of detergent-resistant microdomains under specific stress conditions (Hinderhofer *et al*., 2009; López & Kolter, 2010). Therefore, to expand upon our results with CL we assessed the contribution of the YqiK to the induction, function and spatial organisation of the Psp proteins. Lack of YqiK (Δ*yqiK*; non-polar mutation) does not induce *pspA* per se (Supplementary Fig. S4a) and although with less pronounced effect, reduces the level of induction of *pspA* as also seen in a Δ*cls* mutant (Supplementary Fig. S4a). As a control, we showed the *yqiK* mutation does not impact on deregulated PspF-dependent transcription of *pspA* (Supplementary Fig. S2a) and the over-expression of YqiK did not induce *pspA* (Supplementary Fig. S2b). In line with the morphology of cells expressing YqiK and localisation of YqiK-YFP in *E. coli* (López & Kolter, 2010) our imaging results show that over-expression of YqiK-GFP yields enlarged cells and displays the IM localisations with distinct, relatively static (only local movement is seen) complexes in polar and lateral regions of the cell (Supplementary Fig. S4c, d). The growth of Δ*yqiK* under stress is not substantially different from WT (Supplementary Fig. S4b) and the same are true for sub-cellular localisations of V-PspA (Supplementary Fig. S4e and Video S7). Hence, there are similarities between *cls* and *yqiK* mutants and it seems that YqiK supports signalling for the induction of Psp response.

RodZ affects the Psp response and membrane localisation of V-PspA

The effector function, lateral membrane localisation and dynamics of PspA depend on MreB, while the induction of the Psp response and localisation of PspA regulatory complexes are MreB independent (Engl *et al*., 2009). MreB's circumferential movement along the long axis of the cell is driven by the process of PGL biosynthesis itself (White *et al*., 2010; van Teeffelen et al., 2011; Kawai *et al*., 2011; Garner *et al*., 2011; Dominguez-Escobar *et al*., 2011; v. Olshausen *et al*., 2013) and the association of MreB with the cell wall biosynthesis apparatus is via RodZ protein (Bendezú *et al*., 2009; van den Ent *et al*., 2010).

To address the potential link between PspA and RodZ (via MreB) we assayed activities and spatial distribution of PspA in *rodZ* mutants (Δ*rodZ*, non-polar mutation). We established that the absence of RodZ does not in itself induce *pspA* expression but allows a strong induction of *pspA* upon IM stress which notably is PspBC-independent (Fig. 5a). As controls, lack of RodZ does not influence the PspF-dependent transcription of *pspA* (Supplementary Fig. S2a) and over-expression of RodZ does not induce *pspA* (Supplementary Fig. S2b). However, despite the induction of *pspA* under IM stress being elevated in a Δ*rodZ* mutant, the growth is impaired to an extent seen for the cells lacking a Psp response (Fig. 5b and see Fig. 4c).

In Δ*rodZ* cells with no rod-shape morphology, it is hard to observe distinct V-PspA foci in the absence of IM stress (Fig. 5c). Under stress, the V-PspA expression is induced in Δ*rodZ* cells and we observe distinct dynamic effector complexes (Fig. 5d; Supplementary Video S8). The same is true for plasmid borne eGFP-PspA (Fig. 5e). The movement of eGFP-PspA in Δ*rodZ* cells remains MreB-dependent since in double Δ*mreB* Δ*rodZ* mutant the eGFP-PspA foci are static (Fig. 5f). However, RodZ does contribute to MreB-dependent spatial distribution of eGFP-PspA that may be of importance for the function of the PspA effectors in WT cells. In Δ*mreB* the eGFP-PspA forms distinct static membrane foci (Engl *et al*., 2009 and see Supplementary Fig. S5a) while in double Δ*mreB* Δ*rodZ* mutant the eGFP-PspA foci localise in one membrane macro-domain (Fig. 5f and Supplementary Fig. S5b). Similarly, the eGFP-PspA foci in Δ*mreB* Δ*yqiK* cells lacking MreB and potential flotillin localise in one static horse shoe shaped macro-feature (Supplementary Fig. S5c, d) suggesting MreB, RodZ and YqiK may be involved in organising membrane regions for the intrinsic interactions of PspA complexes with the IM. Interestingly, in plant cells the Vipp1 homologue of PspA was very dynamic under osmotic stress and formed lateral membrane filament-like structures (Zhang *et al*., 2012) resembling those of eGFP-PspA in Δ*mreB* Δ*rodZ* and Δ*mreB* Δ*yqiK* cells.

Notably, even when the cell shape is perturbed, gross regulation of *pspA* transcription is retained. It appears that so long as PspA can localise at the IM then negative control can be relieved. V-PspA

expression is induced by IM stress in Δ*pspBC* Δ*rodZ* cells (Fig. 5g and see also Fig. 5a). Even though the *rodZ* mutants do not have conventional polar membrane regions, the action of PspBC seem to be critical for V-PspA IM localisation since the absence of PspBC in Δ*rodZ* cells causes complete alteration of IM localisations of V-PspA effector complexes. V-PspA then mainly decorates the entire IM (Fig. 5g) suggesting an additional role of PspBC in organising at the IM some PspA effector complexes. Something similar has been observed in cells expressing the eGFP-PspA$_{\Delta 25\text{-}40}$ variant with diminished interaction with PspBC (Jovanovic *et al.*, 2014). The resulting PspA effectors disorganisation we see here in the complete absence of PspBC and when the cell shape is perturbed is even more pronounced.

Block in cell wall synthesis elevates the Psp response to the IM stress and change dynamics of the lateral membrane PspA effectors

To address whether a block in PGL synthesis directly affects the Psp response we treated unstressed or stressed WT cells with different sub-lethal doses of fosfomycin to inhibit bacterial cell wall biogenesis by inactivating the cytoplasmic enzyme MurA that catalyzes the first essential step in PGL biosynthesis (Brown *et al*., 1995). We showed that a short (10 min) addition of fosfomycin, at 1/4 or 1/2 of its minimal inhibitory concentration (MIC), increases the basal level transcription and pIV-dependent stress induction of *pspA* (Fig. 6a). Notably, the corresponding growth of non-stressed cells was better than that of the stressed cells (Fig. 6a). It appears that defective PGL biosynthesis causes an additional IM stress and that may correspondingly account for a Δ*rodZ* mutant elevating the Psp response to pIV (see Fig. 5a and Fig. 6a).

To assess the localisations and dynamics of the V-PspA effectors in stressed WT cells in the presence of fosfomycin we used a wide field SMI. Potentially, a block in PGL biosynthesis could lead to stalling of the membrane V-PspA effectors if their movement is tightly and solely coupled to the cell wall synthesis dynamics via RodZ and MreB. The observed RodZ-independent dynamics of V-PspA and eGFP-PspA (Fig. 5d, e) and MreB-dependent movement of eGFP-PspA (Supplementary Fig. S5a)

suggest that the sub-population of V-PspA should not be affected. Counter-intuitively, fosfomycin treatment (1/2 of MIC, see above) speeds up the diffusion of V-PspA in Δ*pspA* cells producing pIV (average D=0.02 $\mu m^2 s^{-1}$) compared to untreated stressed cells (average D=0.01 $\mu m^2 s^{-1}$) (Fig. 6b). The images show a mixture of cells with normal and more rounded shape (Fig. 6c) found to exhibit 9±0.3 (n=50) V-PspA foci per cell. It is possible PspA has become less constrained in its lateral membrane movements upon block of the PGL synthesis.

DISCUSSION

Peripheral IM-binding proteins are emerging as providing important examples of where their localisations and hence functionalities are directly sensitive to membrane phospholipids composition, membrane curvature and the bacterial cytoskeleton (Foss *et al*., 2011). Here, we established the functional relationships and interdependences between Psp response, bacterial membrane and cytoskeletal elements to provide insights into how cell structure relates to the perception and management of IM stress by PspA.

The IM stress induces strong *psp* expression and consequently we see the formation of high-order oligomeric PspA effectors in polar regions together with an increase of PspA lateral effector complexes (Supplementary Fig. S6). Potentially, the level of the signal and corresponding induction of PspA expression are in correlation with the strength of stimulus and thus also membrane damage. There is growing evidence that the integration of several signals induces the Psp response. Changes in membrane potential leading to a drop in pmf, as well as changes in redox state or mode of respiration were found to be either conditional or not sufficient to signal the IM damage (Jovanovic *et al*., 2009; Wang *et al*., 2010; Engl *et al*., 2011). Particular changes in properties of the membrane are likely to contribute to the origin of the IM stress signal(s) and the sites of PspA effector action. It is clear that there are at least two different pathways involved in IM stress signalling to PspA. One mode employs signal-transduction to the PspA-PspF inhibitory complexes via PspBC sensors and the other acts through a direct binding of PspA-PspF to a stress-related IM determinant (Supplementary Fig. S6).

458 Dual control of the σ^E regulon that responds to outer-membrane stress (Lima *et al*., 2013) has some
459 similarity with the dual modes (PspBC-dependent and PspBC-independent) of IM binding of PspA
460 upon stress.
461
462 Our results connect the CL containing polar regions of the cell with the respective localisations of
463 PspA and PspBC, PspBC signalling, IM-binding of PspA and stress-dependent formation of the high
464 order oligomeric PspA effectors (Supplementary Fig. S6). The PspBC sensors localised in polar
465 regions transduce the IM stress signal(s) to PspA-PspF inhibitory complex releasing negative control
466 of *psp*. PspC may sense a change in IM charge, membrane potential or curvature via CL leading to a
467 switch in PspC topology needed for recruiting PspA to the PspBC complex (Jovanovic *et al*., 2010;
468 Flores-Kim & Darwin, 2012) (see also Supplementary Fig. S6). The protein Opi1 has been shown to
469 exhibits similar behavior with its signalling dependent on intracellular pH and the protonation state of
470 phosphatidic acid phosphate head-groups (Young *et al*., 2010), and for Fis1 binding to lipid vesicles is
471 increased upon protonation and concentration of anionic lipids (Wells & Hill, 2011). The PspBC
472 complex may well integrate the threshold level signals to modulate the Psp response to a range of
473 stimuli. This can lead to reduction of noise and less pronounced oscillations of *psp* induction in
474 agreement with our mechanistic model of the Psp response (Toni *et al*., 2011). Our results also
475 strongly suggest that upon stress in WT cells PspBC are also involved in connecting the PspA effector
476 complex via MreB to particular cell features defined by RodZ, YqiK activities and anionic lipids-rich
477 membrane domains.
478
479 We showed here that the *psp* inducing pIV-originated signal(s), besides using the PspBC signalling
480 pathway, can also act via a PspBC-independent mode. In addition, pIV production in a Δ*rodZ*
481 background (or when PGL biogenesis is blocked) facilitates the IM stress and elevates the importance
482 of the PspBC-independent response. Severe stresses, such as extreme osmotic shock, 50^{o}C
483 temperature, 10% ethanol, have been shown to transiently induce *psp* in PspBC-partial or -
484 independent manner (reviewed in Model *et al*., 1997). Therefore, extreme stimuli may cause PspA to

485 bypass the PspBC signalling and effectively directly respond to changes in the IM (see Supplementary
486 Fig. S6).
487
488 The several lines of evidence suggest that CL-associated protein-translocation systems and adjacent
489 PG-rich domains might be targets for the PspA effector complexes positioned in polar IM regions of
490 the cell (Supplementary Fig. S6). Depletion or defects in all protein translocation systems (Sec, Tat,
491 YidC, SRP) induce PspA (reviewed in Joly *et al*., 2010). Importantly, a PspBC-dependent PspA-Tat
492 interaction (Mehner *et al*., 2012) suggests that the PspA effector function could involve direct repair
493 of the CL-associated translocon system(s). The functions of PspA in repairing Tat defects can be
494 substituted by Vipp1 in *E. coli* while PspA partially substitutes for the same defect in the absence of
495 Vipp1 (DeLisa *et al*., 2004). Moreover, PspA stimulates protein export in *E. coli* (Lleerebezem &
496 Tommassen, 1993) and a PspA homologue improves the pmf-dependent Tat- and Sec-supported
497 heterologous proteins secretion in *Streptomyces* (Vrancken *et al*., 2007). As shown for PspA, the Tat
498 and YidC homologues have been found in bacteria, archaea and chloroplasts. Clade PspA (CL0235)
499 has two members, PspA/IM30 and Snf7. Snf7 is a family of proteins involved in protein sorting and
500 transport from the endosome to the vacuole/lysosome in eukaryotic cells that play an important role in
501 the degradation of both lipids and cellular proteins (Peck *et al*., 2004). Therefore, one major and
502 conserved function of PspA and its homologues may be to maintain the activities of protein
503 translocation systems.
504
505 MreB defines the spatial distribution of lateral membrane PspA effectors and together with its IM
506 binding partner RodZ may be implicated in targeting cell wall synthesis machinery conferring an
507 adaptation of cells to IM stress (Supplementary Fig. S6). Potentially, sites in lateral membrane regions
508 where the cell wall synthesis machinery is assembled can be targeted by MreB-guided PspA effectors
509 in order to possibly support the lipid II-dependent peptidoglycan biosynthesis and elongation of the
510 lateral cell wall under IM stress. On that note, the expression of IM protein MurG, found to interact
511 with MreB and to be essential for lipid II-dependent cycle of PGL synthesis (see Supplementary Fig.
512 S1b) is up-regulated in *E. coli* cells over-expressing PspA (Jovanovic *et al*., 2006). In Gram-positive

513 bacteria lantabiotics and bacitracin interfere with cell wall synthesis by binding lipid II and strongly
514 induce expression of the PspA homologue, LiaH, and its recruitment to membrane (Typas *et al*., 2012;
515 Dominguez-Escobar *et al*., 2014). However, LiaH dynamics in *Bacillus subtilis* was found to be
516 independent on the MreB and cell wall synthesis (Dominguez-Escobar *et al*., 2014).
517
518 The cell wall synthesis machinery in *E. coli* may also serve to attract and functionalise the lateral
519 membrane PspA effectors leading to IM repair upon stress. Genomic analyses showed that RodZ
520 function is conserved and unique to bacteria and that *rodZ* and *pgsA* (required for PG and CL
521 biosyntehsis) genes are often adjacent suggesting they are functionally linked (Alyahya *et al*., 2009).
522 Note that PG has been found to directly bind PspA high-order oligomers which repair membrane
523 damage *in vitro* (Kobayashi *et al*., 2007). Also, gene-to-metabolite correlations suggest that in *E. coli*
524 PG plays a critical role for membrane balance (Takahashi *et al*., 2011). Notably, other envelope
525 associated complexes may well function through MreB and with changes in lipids organisations
526 impact upon the localisations and dynamics of PspA.
527
528 Blocks in lipid biosynthesis induce the expression of PspA (Bergler *et al*., 1994) suggesting that Psp
529 in its effector function(s) may act to modulate lipid metabolism. As observed by using *pspA* or *pspG*
530 mutants or over-expressing PspA or PspG [additional IM effector (Lloyd *et al*., 2004; Jovanovic *et al*.,
531 2006; Engl *et al*., 2009)], these Psp effectors have the potential to diminish the expression of genes
532 implicated in the glycerol shift and aerobic respiration and up-regulate expression of genes that favor
533 Glycerol-3-Phosphate (G3P) conversion into phospholipids (Jovanovic *et al*., 2006; Bury-Mone *et al*.,
534 2009). As we noted above, the increased amount of PG in the Δ*cls* mutant we use here may contribute
535 to the IM stress adaptation when induction of Psp is reduced. Intriguingly, in *E. coli* over-expression
536 of the foreign protein MGS that binds anionic lipids greatly elevates PG production (Ariöz *et al*.,
537 2013) raising the possibility that the IM-binding of highly expressed native PspA effectors may
538 trigger a cellular signal for the stimulation of anionic lipid synthesis to repair and-or exchange the PG
539 (and CL).
540

In summary, the studies presented here show functional link between cardiolipin, PspBC-dependent signalling and polar IM localisation of the PspA. Upon IM stress the PspA regulator switches to high-order oligomeric effector complexes in polar regions of the cell whilst employing bacterial actin MreB to target lateral membrane regions, some of which are marked by cell wall biosynthesis machinery protein RodZ. Further experiments are needed to reveal which properties of the IM change in a stress-specific manner to directly signal the membrane stress to PspA and to unravel the molecular mechanism of IM repair.

ACKNOWLEDGEMENTS

This work was funded by BBSRC and Leverhulme Trust project grants. We acknowledge A. Bruckbauer and A. Vaahtokari (London Research Institute, Cancer Research UK) for support at the Super-Resolution Microscopy Core Facility, T. Lenn for technical help, Y.-L. Shih for MC1000 and MC1000 Δ*mreB* strains, and M. Russel for plasmid pMJR129. We thank J. Dworkin (Columbia University) for advice and members of the M. Buck laboratory for critical reading and comments on the manuscript.

REFERENCES

Alyahya, S. A., Alexander, R., Costa, T., Henriques, A. O., Emonet, T. & Jacobs-Wagner, C. (2009). RodZ, a component of the bacterial core morphogenic apparatus. *Proc Natl Acad Sci U S A* **106**, 1239-1244.

Arias-Cartin, R., Grimaldi, S., Arnoux, P., Guigliarelli, B. & Magalon, A. (2012). Cardiolipin binding in bacterial respiratory complexes: structural and functional implications. *Biochim Biophys Acta* **1817**, 1937-1949.

Ariöz, C., Ye, W., Bakali, A., Ge, C., Liebau, J., Götzke, H., Barth, A., Wieslander, Å. & Mäler, L. (2013). Anionic lipid binding to the foreign protein MGS provides a tight coupling between phospholipid synthesis and protein overexpression in *Escherichia coli*. *Biochemistry* **52**, 5533-5544.

Aseeva, E., Ossenbühl, F., Eichacker, L. A., Wanner, G., Soll, J. & Vothnecht U. C. (2004). Complex formation of Vipp1 depends on it's α-helical PspA-like domain. *J Biol Chem* **279**, 35535-35541.

Aseeva, E., Ossenbühl, F., Sippel, C., Cho, W. K., Stein, B., *et al*. (2007). Vipp1 is required for basic thylakoid membrane formation but not for the assembly of thylakoid protein complexes. *Plant Physiol Bioch* **45**, 119–128.

Bach, J. N. & Bramkamp M. (2013). Flotillins functionally organise the bacterial membrane. *Mol Microbiol* **88**, 1205-1217.

Barák, I., Muchova, K., Wilkinson, A. J., O'Toole, P. J. & Pavlendová, N. (2008). Lipid spirals in *Bacillus subtilis* and their role in cell division. *Mol Microbiol* **68**, 1315-1327.

Bendezú, F. O., Hale, C. A., Bernhardt, T. G. & de Boer, P. A. (2009). RodZ (YfgA) is required for proper assembly of the MreB actin cytoskeleton and cell shape in *E. coli*. *EMBO J* **28**, 193-204.

Bergler, H., Abraham, D., Aschauer, H. & Turnowsky, F. (1994). Inhibition of lipid biosynthesis induces the expression of the *pspA* gene. *Microbiology* **140**, 1937-1944.

Berthelmann, F. & Brüser, T. (2004). Localization of the Tat translocon components in *Escherichia coli*. *FEBS Lett* **569**, 82-88.

Brown, E. D., Vivas, E. I, Walsh, C. T. & Kolter, R. (1995). MurA (MurZ), the enzyme that catalyzes the first committed step in peptidoglycan biosynthesis, is essential in *Escherichia coli*. *J Bacteriol* **177**, 4194–4197.

Bury-Mone, S., Nomane, Y., Reymond, N., Barbet, R., Jacquet, E., Imbeaud, S., Jacq, A. & Bouloc, P. (2009). Global analysis of extracytoplasmic stress signalling in *Escherichia coli*. *PLoS Genet* **5**, e1000651.

Darwin, A. J. (2005). The phage-shock-protein response. *Mol Microbiol* **57**, 621-628.

Darwin, A. J. (2013). Stress relief during host infection: the phage shock protein response supports bacterial virulence in various ways. *PLoS Pathog* **9**, e1003388.

DeLisa, M. P., Lee, P., Palmer, T. & Georgiou, G. (2004). Phage shock protein PspA of *Escherichia coli* relieves saturation of protein export via the Tat pathway. *J Bacteriol* **186**, 366–373.

Dhamdhere, G. & Zgurskaya, H. I. (2010). Metabolic shutdown in *Escherichia coli* cells lacking the outer membrane channel TolC. *Mol Microbiol* **77**, 743–754.

Domínguez-Escobar, J., Chastanet, A., Crevenna, A. H., Fromion, V., Wedlich-Söldner, R. & Carballido-López, R. (2011). Processive movement of MreB-associated cell wall biosynthetic complexes in bacteria. *Science* **333**, 225-228.

Domínguez-Escobar, J., Wolf, D., Fritz, G., Höfler, C., Wedlich-Söldner, R. & Mascher, T. (2014). Subcellular localization, interactions and dynamics of the phage shock protein-like Lia response in *Bacillus subtilis*. *Mol Microbiol* **92**, 716-732.

Donovan, C. & Bramkamp, M. (2009). Characterization and subcellular localization of a bacterial flotillin homologue. *Microbiology* **155**, 1786-1799.

Engl, C., Beek, A. T., Bekker, M., de Mattos, J.T., Jovanovic, G. & Buck, M. (2011). Dissipation of proton motive force is not sufficient to induce the phage shock protein response in *Escherichia coli*. *Curr Microbiol* **62**, 1374-1385.

Engl, C., Jovanovic, G., Lloyd, L. J., Murray, H., Ying, L., Errington, J. & Buck, M. (2009). *In vivo* localizations of membrane stress controllers PspA and PspG in *Escherichia coli*. *Mol Microbiol* **73**, 382-396.

Flores-Kim, J. & Darwin, A. J. (2012). Phage shock protein C (PspC) of *Yersinia enterocolitica* is a polytopic membrane protein with implications for regulation of the Psp stress response. *J Bacteriol* **194**, 6548-6559.

Foss, M. H., Eun, Y-J. & Weibel, D. B. (2011). Chemical-biological studies of subcellular organization in bacteria. *Biochemistry* **50**, 7719-7734.

Garner, E. C., Bernard, R., Wang, W., Zhuang, X., Rudner, D. Z. & Mitchison, T. (2011). Coupled, circumferential motions of the cell wall synthesis machinery and MreB filaments in *B. subtilis*. *Science* **333**, 222-225.

Hinderhofer, M., Walker, C. A., Friemel, A., Stuermer, C. A. O., Möller, H. M. & Reuter, A. (2009). Evolution of prokaryotic SPFH proteins. *BMC Evol Biol* **9**, 22.

Horstman, N. K. & Darwin, A. J. (2012). Phage shock proteins B and C prevent lethal cytoplasmic membrane permeability in *Yersinia enterocolitica*. *Mol Microbiol* **85**, 445-460.

Huvet, M., Toni, T., Sheng, X., Thorne, T., Jovanovic, G., Engl, C., Buck, M., Pinney, J. W. & Stumpf, M. P. H. (2011). The evolution of the phage shock protein response system: interplay between protein function, genomic organization, and system function. *Mol Biol Evol* **28**, 1141-1155.

Joly, N., Burrows, P. C., Engl, C., Jovanovic, G. & Buck, M. (2009). A lower-order oligomer form of phage shock protein A (PspA) stably associates with the hexameric AAA^+ transcription activator protein PspF for negative regulation. *J Mol Biol* **34**, 764-775.

Joly, N., Engl, C., Jovanovic, G., Huvet, M., Toni, T., Sheng, X., Stumpf, M. P. H. & Buck, M. (2010). Managing membrane stress: the phage shock protein (Psp) response, from molecular mechanisms to physiology. *FEMS Microbiol Rev* **34**, 797-827.

Jovanovic, G., Engl, C. & Buck, M. (2009). Physical, functional and conditional interactions between ArcAB and phage shock proteins upon secretin-induced stress in *Escherichia coli*. *Mol Microbiol* **74**, 16-28.

Jovanovic, G., Engl, C., Mayhew, A. J., Burrows, P. C. & Buck, M. (2010). Properties of the phage-shock- protein (Psp) regulatory complex that govern signal transduction and induction of the Psp response in *Escherichia coli*. *Microbiology* **156**, 2920-2932.

Jovanovic, G., Lloyd, L. J., Stumpf, M. P. H., Mayhew, A. J. & Buck, M. (2006). Induction and function of the phage shock protein extracytoplasmic stress response in *Escherichia coli*. *J Biol Chem* **281**, 21147-21161.

Jovanovic, G., Mehta, P., McDonald, C., Davidson, A. C., Uzdavinys, P., Ying, L. & Buck, M. (2014). The N-terminal amphipathic helices determine regulatory and effector functions of phage shock protein A (PspA) in *Escherichia coli*. *J Mol Biol* **426**, 1498-1511.

Kawai, Y., Marles-Wright, J., Cleverley R. M., Emmins, R., Ishikawa, S., *et al*. (2011). A widespread family of bacterial cell wall assembly proteins. *EMBO J* **30**, 4931-4941.

Kleerebezem, M. & Tommassen, J. (1993). Expression of the *pspA* gene stimulates efficient protein export in *Escherichia coli*. *Mol Microbiol* **7**, 947–956.

Kobayashi, R., Suzuki, T. & Yoshida, M. (2007). *Escherichia coli* phage-shock protein A (PspA) binds to membrane phospholipids and repairs proton leakage of the damaged membranes. *Mol Microbiol* **66**, 100-109.

Lenn, T., Gkekas, C. N., Bernard, L., Engl, C., Jovanovic, G., Buck, M. & Ying, L. (2011). Measuring the stoichiometry of functional PspA complexes in living bacterial cells by single molecule photobleaching. *Chem Comm* **47**, 400-402.

Lima, S., Guo, M. S., Chaba, R., Gross, C. A. & Sauer, R. T. (2013). Dual molecular signals mediate the bacterial response to outer-membrane stress. *Science* **340**, 837-841.

Lloyd, L. J., Jones, S. E., Jovanovic, G., Gyaneshwar, P., Rolfe, M. D., Thompson, A., *et al.* (2004). Identification of a new member of the phage shock protein response in *Escherichia coli*, the phage shock protein G (PspG). *J Biol Chem* **279**, 55707-55714.

López, D. & Kolter, R. (2010). Functional microdomains in bacterial membranes. *Genes Dev* **24**, 1893-1902.

Mehner, D., Osadnik, H., Lünsdorf, H. & Brüser, T. (2012). The Tat system for membrane translocation of folded proteins recruits the membrane-stabilizing Psp machinery in *Escherichia coli*. *J Biol Chem* **287**, 27834-27842.

Mehta, P., Jovanovic, G., Lenn, T., Bruckbauer, A., Engl, C., Ying, L. & Buck, M. (2013). Localisations, dynamics and stoichiometry of a regulated enhancer-binding protein in live *Escherichia coli* cells. *Nat Commun* **4**, 1997.

Miller, J. H. (1992). *A short course in Bacterial Genetics: a laboratory manual and handbook for* Escherichia coli *and related bacteria*. Cold Spring Harbor, NY: Cold Spring Harbor Laboratory

Model, P., Jovanovic, G. & Dworkin, J. (1997). The *Escherichia coli* phage-shock-protein (*psp*) operon. *Mol Microbiol* **24**, 255-261.

Peck, J. W., Bowden, E. T. & Burbelo, P. D. (2004). Structure and function of human Vps20 and Snf7 proteins. *Biochem J* **377**, 693-700.

Raetz C. R. H. (1986). Molecular genetics of membrane phospholipid synthesis. *Ann Rev Genet* **20**, 253-295.

Renner, L. D. & Weibel, D. B. (2011). Cardiolipin microdomains localize to negatively curved regions of *Escherichia coli* membranes. *Proc Natl Acad Sci U S A* **108**, 6264-6269.

Salje, J., van den Ent, F., de Boer, P. & Löwe, J. (2011). Direct membrane binding by bacterial actin MreB. *Cell* **43**, 478-487.

Takahashi, H., Morioka, R., Ito, R., Oshima, T., Altaf-Ul-Amin, Md., Ogasawara, N. & Kanaya, S. (2011). Dynamics of time-lagged gene-to-metabolite networks of *Escherichia coli* elucidated by integrative Omics approach. *OMICS* **215**, 15–23.

Tan, B. K., Bogdanov, M., Zhao, J., Dowhan, W., Raetz, C. R. H. & Guan, Z. (2012). Discovery of a cardiolipin synthase utilizing phosphatidylethanolamine and phosphatidylglycerol as substrates. *Proc Natl Acad Sci U S A* **109**, 16504-16509.

Toni, T., Jovanovic, G., Huvet, M., Buck, M. & Stumpf, M. P. H. (2011). From qualitative data to quantitative models: analysis of the phage shock protein stress response in *Escherichia coli*. *BMC Syst Biol* **5**, 69.

Typas, A., Banzhaf, M., Gross, C. A. & Vollmer, W. (2012). From the regulation of peptidoglycan synthesis to bacterial growth and morphology. *Nat Rev Microbiol* **10**, 123-136.

v. Olshausen, P., Soufo, H. J. D., Wicker, K., Heintzmann, R., Graumann, P. L. & Rohrbach, A. (2013). Superresolution imaging of dynamic MreB filaments in B. subtillis–A multiple-motor-driven transport? *Biophys J* **105**, 1171-1181.

van den Ent, F., Johnson, C. M., Persons, L., de Boer, P. & Löwe, J. (2010). Bacterial actin MreB assembles in complex with cell shape protein RodZ. *EMBO J* **29**, 1081-1090.

van Teeffelen, S., Wang, S., Furchtgott, L., Huang, K. C., Wingreen, N. S., Shaevitz, W. & Gitai, Z. (2011). The bacterial actin MreB rotates, and rotation depends on cell-wall assembly. *Proc Natl Acad Sci U S A* **108**, 15822-15827.

Vega, N. M., Allison, K. R., Samuels, A. N., Klempner, M. S. & Collins J. J. (2013). *Salmonella typhimurium* intercepts *Escherichia coli* signalling to enhance antibiotic tolerance. *Proc Natl Acad Sci U S A* **110**, 14420-14425.

Vothknecht, U. C., Otters, S., Hennig, R. & Schneider, D. (2012). Vipp1: a very important protein in plastids?! *J Exp Bot* **63**, 1699-1712.

Vrancken, K., De Keersmaeker, S., Geukens, N., Lammertyn, E., Anne, J. & VanMellaert, L. (2007). *pspA* overexpression in *Streptomyces lividans* improves both Sec- and Tat-dependent protein secretion. *Appl Microbiol Biot* **73**, 1150–1157.

Wallrodt, I., Jelsbak, L., Thomsen, L. E., Brix, L., Lemire, S., Gautier, L., Nielsen, D. S., Jovanovic, G., Buck, M. & Olsen, J. E. (2014). Removal of the phage shock protein PspB causes reduction of virulence in Salmonella enterice serovar Typhimurium independently of NRAMP1. J Med Microbiol **63**, 788-795.

Wang, P., Kuhn, A. & Dalbey, R. E. (2010). Global change of gene expression and cell physiology in YidC-depleted *Escherichia coli*. *J Bacteriol* **192**, 2193–2209

Wells, R. C. & Hill, R. B. (2011). The cytosolic domain of Fis1 binds and reversibly clusters lipid vesicles. *PLoS ONE* **6**, e21384.

Westphal, S., Heins, L., Soll, J. & Vothknecht, U. C. (2001). *Vipp1* deletion mutant of *Synechocystis*: a connection between bacterial phage shock and thylakoid biogenesis? *Proc Natl Acad Sci U S A* **98**, 4238-4242.

White, C. L., Kitich, A. & Gober, J. W. (2010). Positioning cell wall synthetic complexes by the bacterial morphogenetic proteins MreB and MreD. *Mol Microbiol* **76**, 616-633.

White, M. J., Savaryn, J. P., Bretl, D. J., He, H., Penoske, R. M., Terhune, S. S. & Zahrt, T. C. (2011). The HtrA-like serine protease PepD interacts with and modulates the *Mycobacterium tuberculosis* 35-kDa antigen outer envelope protein. *PLoS ONE* **6**, e18175.

Wickström, D., Wagner, S., Baars, L., Ytterberg, A. J., Klepsch, M., van Wijk, K. J., Luirink, J. & de Gier, J-W. (2011). Consequences of depletion of the signal recognition particle in *Escherichia coli*. *J Biol Chem* **286**, 4598-4609.

Yamaguchi, S. & Darwin, A. J. (2012). Recent findings about the *Yersinia enterocolitica* phage shock protein response. *J Microbiol* **50**, 1-7.

Yamaguchi, S., Dylan, A. R., Rothenberg, E. & Darwin A. J. (2013). Changes in Psp protein binding partners, localization and behavior upon activation of the *Yersinia enterocolitica* phage shock protein response. *Mol Microbiol* **87**, 656-671.

Yamaguchi, S., Gueguen, E., Horstman, N. K. & Darwin, A. J. (2010). Membrane association of PspA depends on activation of the phage-shock-protein response in *Yersinia enterocolitica*. *Mol Microbiol* **78**, 429-443.

Young, B. P., Shin, J. J. H., Orij, R., Chao, J. T., Li, S. C., *et al*. (2010). Phosphatidic acid is a pH biosensor that links membrane biogenesis to metabolism. *Science* **329**, 1085-1088.

Zhang, L., Kato, Y., Otters, S., Vothknecht, U. C. & Sakamoto, W. (2012). Essential role of Vipp1 in chloroplast envelope maintenance in *Arabidopsis*. *Plant Cell* **24**, 3695-707.

Zhang, L. & Sakamoto, W. (2013). Possible function of VIPP1 in thylakoids. *Plant Signal Behav* **8**, e22860.

Zhang, N., Simpson, T., Lawton, E., Uzdavinys, P., Joly, N., Burrows, P. & Buck, M. (2013). A key hydrophobic patch identified in an AAA^+ protein essential for *in trans* inhibitory regulation. *J Mol Biol* **425**, 2656-2669.

FIGURE LEGENDS

Fig. 1. The IM stress dependent sub-cellular distribution of V-PspA. **(a)** Construct expressing chromosomal V-PspA under control of the *pspA* promoter (P_{pspA}) in a Δ*pspA* strain (MVA127). **(b)** Wide field SMI of MVA127 cells expressing V-PspA (white foci) in the absence of stress (+vector, pGZ119EH, after 20 min) and **(c)** upon stress (+pIV-cam, pMJR129) with pIV expression induced for 10 min or **(d)** for 20 min before imaging. **(e)** Wide field SMI of eGFP-PspA (pEC1) in a non-stressed Δ*pspA* (MG1655Δ*pspA*). (b-e): Representative images are shown. Bar, 1 μm. Schematics represent non-quantitative interpretations of the images depicting localisations and dynamics of V-PspA or eGFP-PspA: black dot, membrane foci; gray dot, less frequently observed membrane foci; arrow, dynamic membrane foci. **(f)** Western blot to show the level of pIV expression (band~46 kDa) in cells from (c, d) and control pIV level in cells at 0 time point without IPTG (-). LC, loading control is the protein band from crude cell extract that shows the non-specific cross-reaction with the pIV antibody (α-pIV). M, molecular weight marker. Below: The quantification of pIV protein levels presented in arbitrary units. **(g)** Left hand: Graph of total fluorescence intensity of V-PspA and eGFP-PspA foci (n=50) from (b-e). Right hand: Lateral membrane (M-lateral) localisation of the V-PspA foci (n=50) from (b-d) and eGFP-PspA foci (n=50) from (e) on x-axis and percentage of all foci analysed on y-axis.

832 **Fig. 2.** The stoichiometry of V-PspA before and after IM stress. Determining the stoichiometry by
833 photobleaching of the V-PspA in MVA127 cells: the distribution of stoichiometries calculated from
834 data obtained for V-PspA: **(a)** nucleoid-associated foci (non-stress, n=14) and **(b)** polar IM-associated
835 foci under non-stress (n=66) or stress (+pIV, pGJ4; n=67). Schematics (as in Fig. 1): circle, nucleoid-
836 associated foci; black dot, membrane foci; arrow, dynamic membrane foci.
837
838 **Fig. 3.** The negative control of *psp* and spatial distribution of V-PspA. **(a)** Construct expressing
839 chromosomal V-PspA under control of the *pspA* promoter (P_{pspA}) in a $pspA^+$ cells (MVA101). **(b)** Left
840 hand: Western blot to show the V-PspA fusion (~53 kDa) stability and expression in MVA101 before
841 and after stress (+pIV, pGJ4). α-GFP JL8, Venus antibodies; M, molecular weight marker. Middle:
842 LC, loading control, Coomassie stained MVA101-/+pIV samples. Right hand: The quantification of
843 V-PspA protein expression presented in arbitrary units. **(c)** Wide field SMI of non-stressed MVA101
844 cells expressing V-PspA and **(d)** with induced expression of V-PspA upon stress (+pIV, pGJ4). (c, d):
845 Representative images are shown. Bar, 1 μm. Schematics (as in Fig. 1): circle, nucleoid-associated
846 foci; black dot, membrane foci; arrow, dynamic membrane foci.
847
848 **Fig. 4.** Cardiolipin as a determinant in IM stress signalling to PspA. **(a)** The activity of P*pspA* in WT
849 (MVA44), Δ*pspBC* (MVA45), Δ*cls* (MVA116), and Δ*pspBC* Δ*cls* (MVA117) cells under non-stress
850 (vector pBR325D) or stress (+pIV, pGJ4) conditions. **(b)** Growth of the WT (MG1655) and Δ*cls*
851 (MVA115) cells under non stress (+vector) or stress (+pIV) conditions. **(c)** Growth of the Δ*pspF*
852 mutant (MG1655Δ*pspF*) under non stress or stress conditions as in b. b-c, the experiments are done in
853 triplicate and representative results are presented. Growth of Δ*cls*+pIV and Δ*pspF*+pIV are
854 significantly different from corresponding non-stressed or WT non-stressed or stressed cells (for
855 Δ*cls*+pIV, $P<0.001$; for Δ*pspF*+pIV, $P<0.02$) as determined by one sample t-test analysis of ODs. **(d-**
856 **f)** Wide field SMI of V-PspA expressed in d - Δ*cls* (MVA118) in the absence of pIV (loss of polar
857 foci) e – WT (MVA101) and Δ*cls* under stress (+pIV) (note loss of polar foci) and f - Δ*pspBC* Δ*cls*
858 (MVA119) under stress (+pIV). (d-f): Representative images are shown. Bar, 1 μm. Schematics (as in

Fig. 1): circle, nucleoid-associated foci; black dot, membrane foci; gray dot, less frequently observed membrane foci; arrow, dynamic membrane foci. **(g)** Sub-cellular localisations of the V-PspA foci from (e) on x-axis (M-lateral, lateral membrane; M-polar, polar membrane region) and percentage of all foci analysed (n=115 for WT+pIV, Δ*cls*+pIV) on y-axis.

Fig. 5. Expression, localisation and effector function of PspA in *rodZ* mutants. **(a)** The expression of P*pspA* under non-stress (vector pBR325D) or stress (+pIV, pGJ4) conditions measured in WT (MVA44), Δ*pspBC* (MVA45), Δ*rodZ* (MVA108) and Δ*pspBC* Δ*rodZ* (MVA109) cells. **(b)** Growth of the WT (MG1655) and Δ*rodZ* mutant (MVA105) under non stress (+vector) and stress (+pIV) conditions (the experiment is done in triplicate; a representative result is presented). Growth of Δ*rodZ*+pIV is significantly different from corresponding non-stressed or WT non-stressed or stressed strains ($P<0.04$) as determined by one sample t-test analysis of OD values. **(c, d)** Wide field SMI of V-PspA expressed in a Δ*rodZ* (MVA110) strain: c - non-stress or d - stress (+pIV). **(e)** The localisation of the eGFP-PspA (pEC1) in Δ*rodZ* (MVA105) cells resembles V-PspA+pIV localisations and dynamics in Δ*rodZ* (in d). (f) The localisations and dynamics of eGFP-PspA in Δ*rodZ* is MreB dependent. **(g)** Images of V-PspA in Δ*pspBC* Δ*rodZ* (MVA111) cells –upon stress (+pIV; note decoration of the IM with the V-PspA). (c-g): Representative images are shown. Bar, 1 μm. Schematics (as in Fig. 1): black dot, membrane foci; gray dot, less frequently observed membrane foci; arrow, dynamic membrane foci; black shape, foci arranged in macro domain; black circle, foci decorate the membrane. .

Fig. 6. Fosfomycin treatment increases IM stress and dynamics of V-PspA. **(a)** The expression of P*pspA* was determined in three independent experiments (i-iii) in WT+vector (MVA44+pBR325D, grey) and stressed WT+pIV (MVA44+pGJ4, dark grey) cells in the absence (0) or presence of fosfomycin in different concentrations (1/x) where 1 represents MIC (64 μg ml^{-1}) (See Methods for details). The expression of *pspA* in non-stressed or stressed cells treated with fosfomycin is significantly different from untreated cells (non-stressed $P<0.01$, stressed $P<0.005$) as determined by

one sample t-test analysis of [MU]. Below are corresponding ODs of non-stressed (i-iii thin line) and stressed (i-iii in bold) cells in the absence or presence of fosfomycin. **(b)** The distribution of diffusion coefficients for V-PspA in Δ*pspA* cells (MVA127) under stress (+pIV, pGJ4) and in the absence (in white, n=709) or presence (in grey, n=1106) of 32 μg ml^{-1} of fosfomycin (1/2 MIC) after 10 min of growth. The data are presented as normalised distributions of the diffusion coefficients ($\mu m^2 s^{-1}$) obtained as described (Mehta *et al*., 2013). **(c)** Example of wide field SMI of V-PspA in Δ*pspA* cells under stress and in the presence of fosfomycin as in b. Bar, 1 μm.

Figure 1

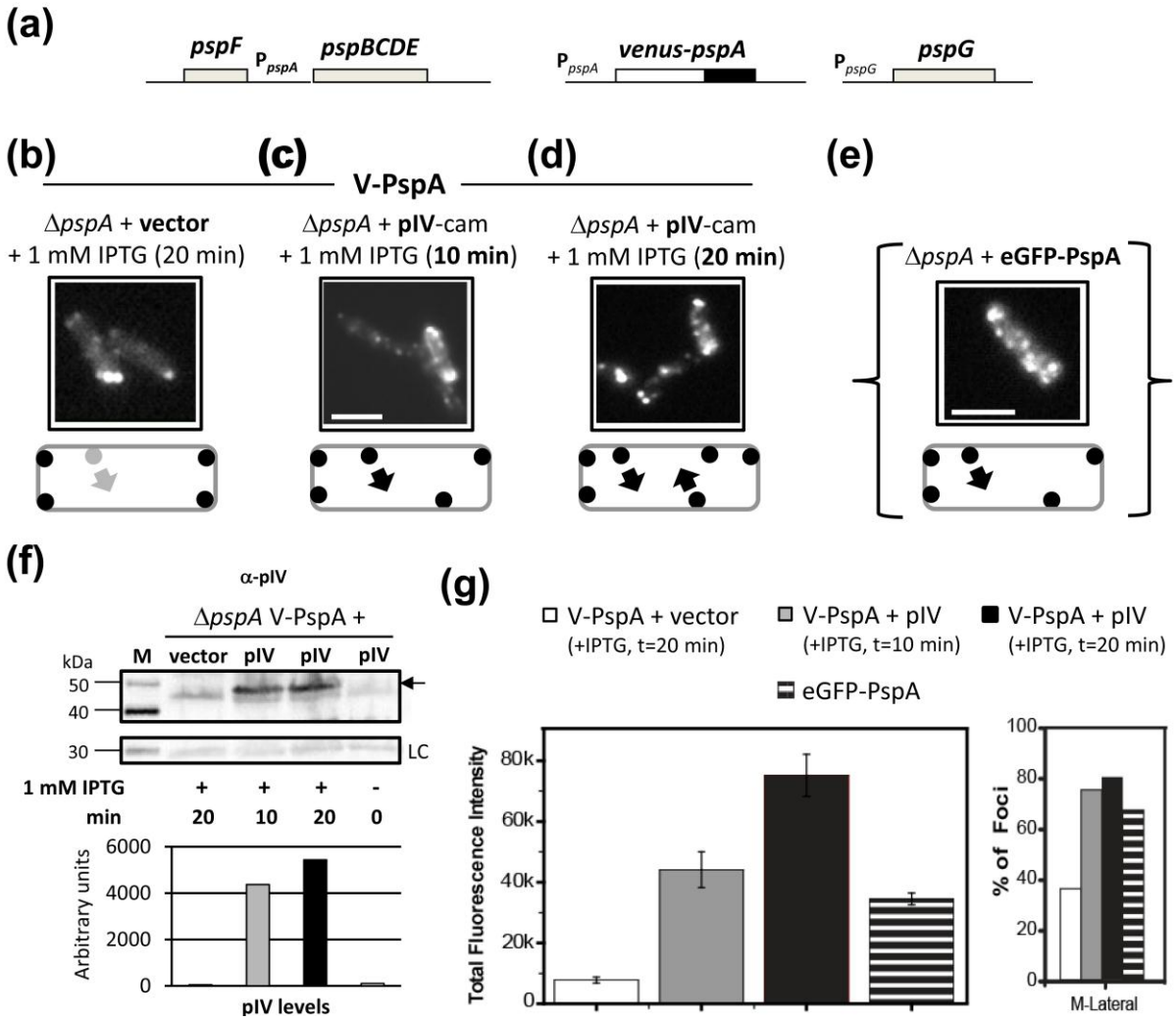
(a)
pspF
P pspA
pspBCDE
P pspA
venus-pspA
P pspG
pspG
(b)
(c)
V-PspA
(d)
(e)
ΔpspA + vector
+ 1 mM IPTG (20 min)
ΔpspA + pIV-cam
+ 1 mM IPTG (10 min)
ΔpspA + pIV-cam
+ 1 mM IPTG (20 min)
ΔpspA + eGFP-PspA
(f)
α-pIV
ΔpspA V-PspA +
kDa
M
vector
pIV
pIV
pIV
50
40
30
LC
1 mM IPTG
+
+
+
-
min
20
10
20
0
Arbitrary units
6000
4000
2000
0
pIV levels
(g)
V-PspA + vector
(+IPTG, t=20 min)
V-PspA + pIV
(+IPTG, t=10 min)
V-PspA + pIV
(+IPTG, t=20 min)
eGFP-PspA
Total Fluorescence Intensity
80k
60k
40k
20k
0
% of Foci
100
80
60
40
20
0
M-Lateral

Figure 2

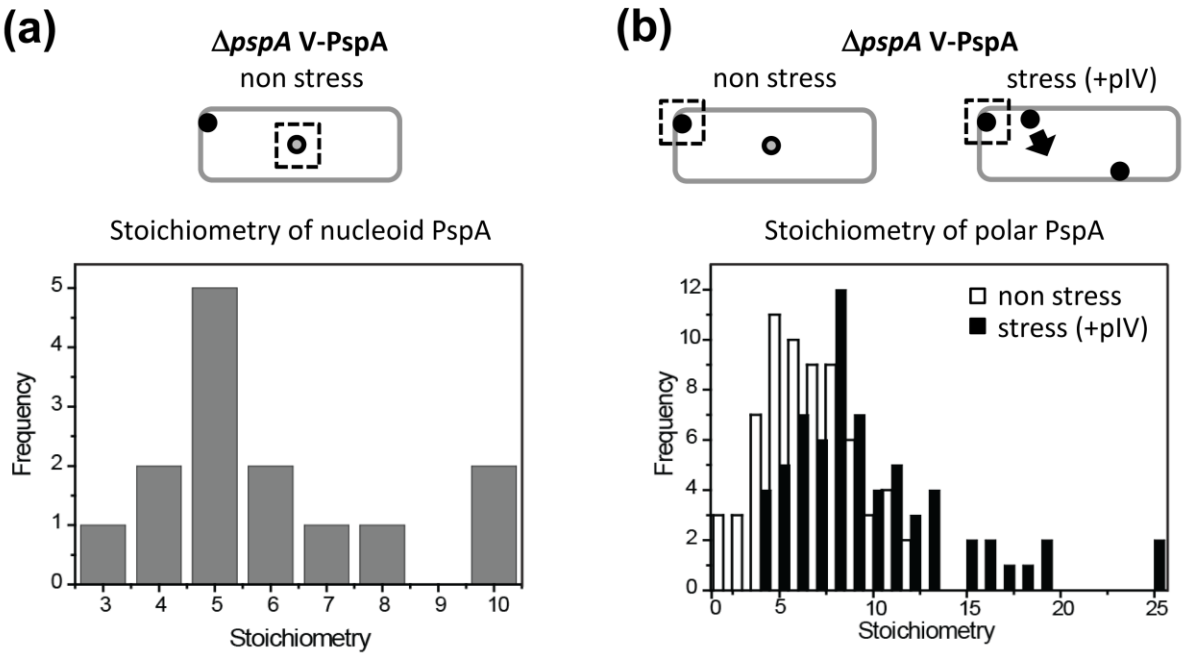
(a)
ΔpspA V-PspA
non stress
Stoichiometry of nucleoid PspA
Frequency
Stoichiometry
(b)
ΔpspA V-PspA
non stress
stress (+pIV)
Stoichiometry of polar PspA
non stress
stress (+pIV)
Frequency
Stoichiometry

Figure 3

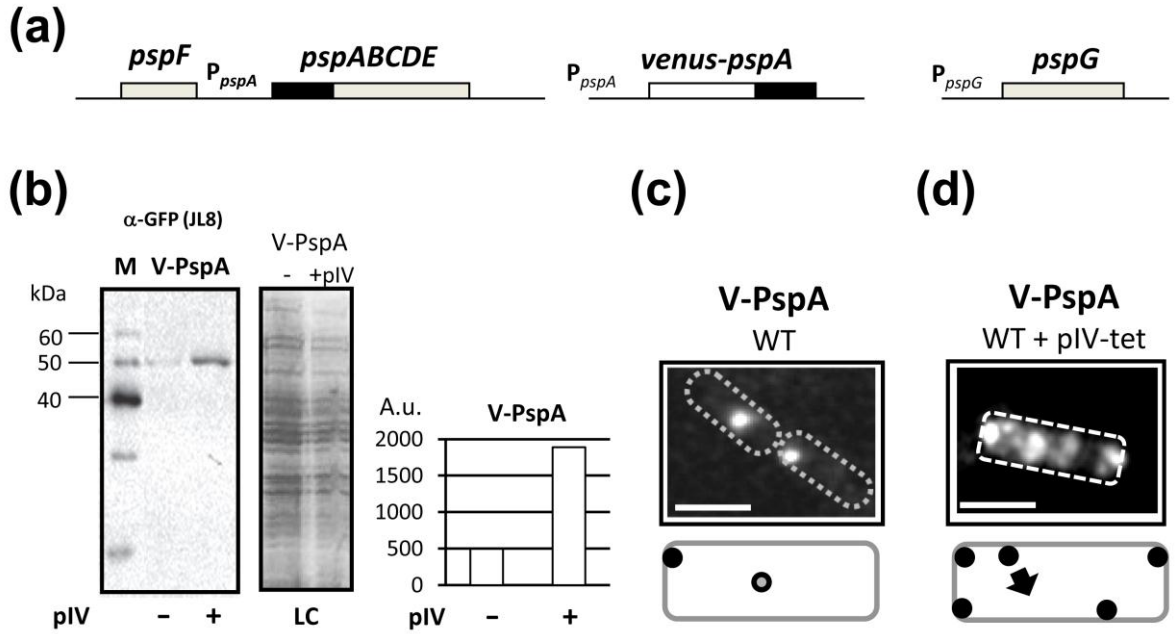
(a)
pspF
P pspA
pspABCDE
P pspA
venus-pspA
P pspG
pspG
(b)
α-GFP (JL8)
M V-PspA
kDa
60
50
40
pIV – +
V-PspA
- +pIV
LC
A.u.
V-PspA
2000
1500
1000
500
0
pIV – +
(c)
V-PspA
WT
(d)
V-PspA
WT + pIV-tet

Figure 4

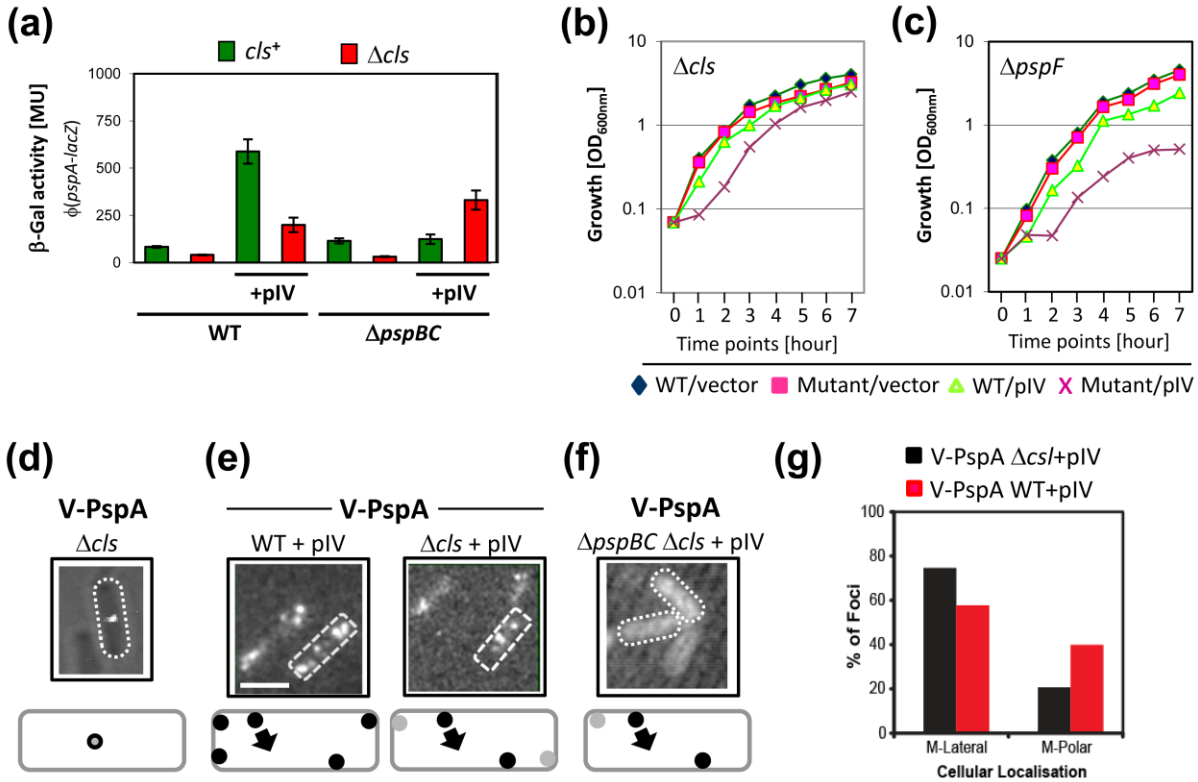
(a)
cls+
Δcls
β-Gal activity [MU]
ϕ(pspA-lacZ)
1000
750
500
250
0
+pIV
+pIV
WT
ΔpspBC
(b)
Δcls
Growth [OD600nm]
10
1
0.1
0.01
0 1 2 3 4 5 6 7
Time points [hour]
(c)
ΔpspF
Growth [OD600nm]
10
1
0.1
0.01
0 1 2 3 4 5 6 7
Time points [hour]
WT/vector
Mutant/vector
WT/pIV
Mutant/pIV
(d)
V-PspA
Δcls
(e)
V-PspA
WT + pIV
Δcls + pIV
(f)
V-PspA
ΔpspBC Δcls + pIV
(g)
V-PspA Δcsl+pIV
V-PspA WT+pIV
% of Foci
100
80
60
40
20
0
M-Lateral
M-Polar
Cellular Localisation

Figure 5

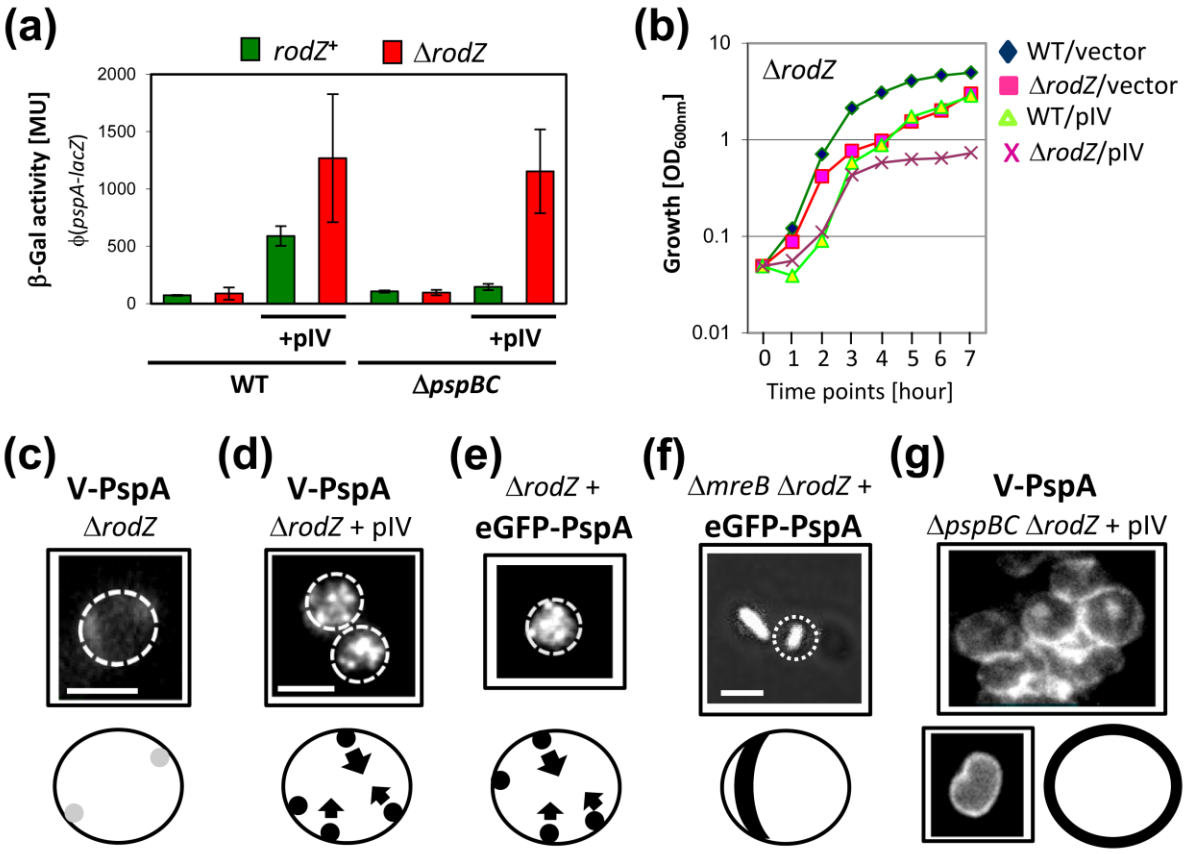
(a)
rodZ+
ΔrodZ
β-Gal activity [MU]
ϕ(pspA-lacZ)
2000
1500
1000
500
0
+pIV
+pIV
WT
ΔpspBC
(b)
ΔrodZ
Growth [OD600nm]
10
1
0.1
0.01
0 1 2 3 4 5 6 7
Time points [hour]
WT/vector
ΔrodZ/vector
WT/pIV
ΔrodZ/pIV
(c)
V-PspA
ΔrodZ
(d)
V-PspA
ΔrodZ + pIV
(e)
ΔrodZ +
eGFP-PspA
(f)
ΔmreB ΔrodZ +
eGFP-PspA
(g)
V-PspA
ΔpspBC ΔrodZ + pIV

Figure 6

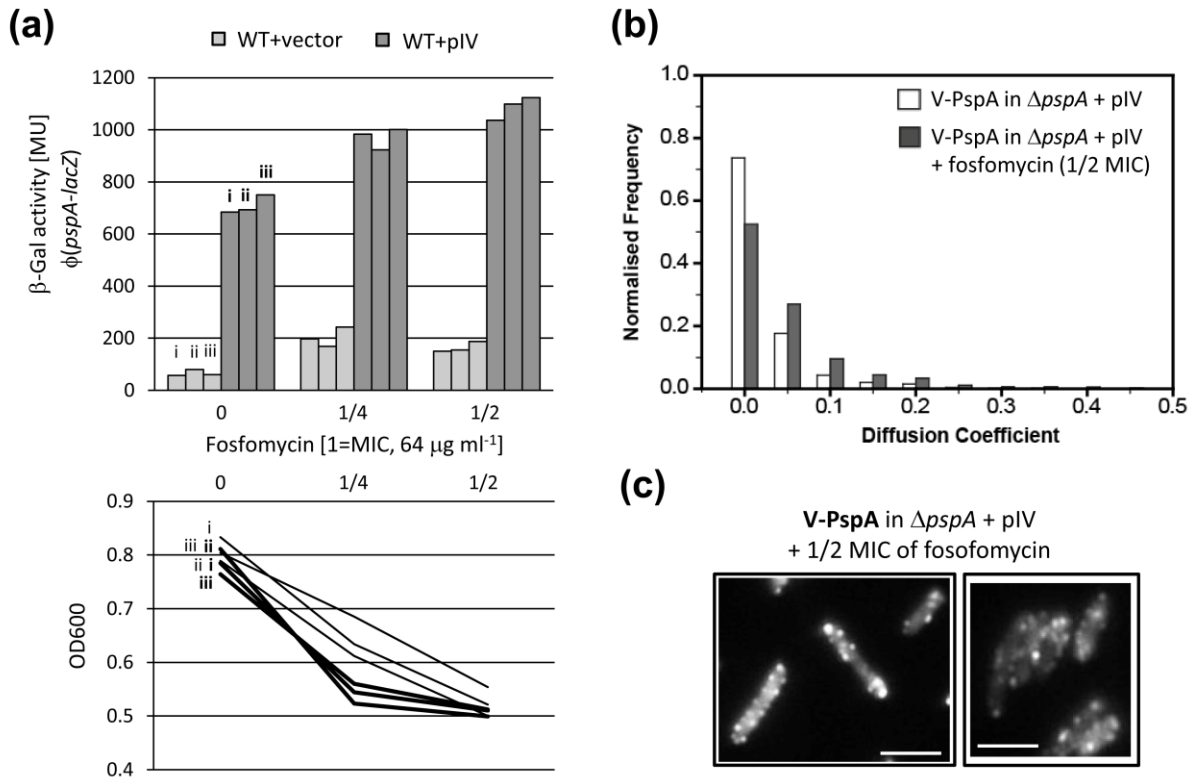
(a)
WT+vector
WT+pIV
β-Gal activity [MU]
ϕ(pspA-lacZ)
1200
1000
800
600
400
200
0
i ii iii
i ii
iii
0
1/4
1/2
Fosfomycin [1=MIC, 64 μg ml-1]
0
1/4
1/2
OD600
0.9
0.8
0.7
0.6
0.5
0.4
i
iii ii
ii i
iii
(b)
V-PspA in ΔpspA + pIV
V-PspA in ΔpspA + pIV
+ fosfomycin (1/2 MIC)
Normalised Frequency
1.0
0.8
0.6
0.4
0.2
0.0
0.0
0.1
0.2
0.3
0.4
0.5
Diffusion Coefficient
(c)
V-PspA in ΔpspA + pIV
+ 1/2 MIC of fosofomycin